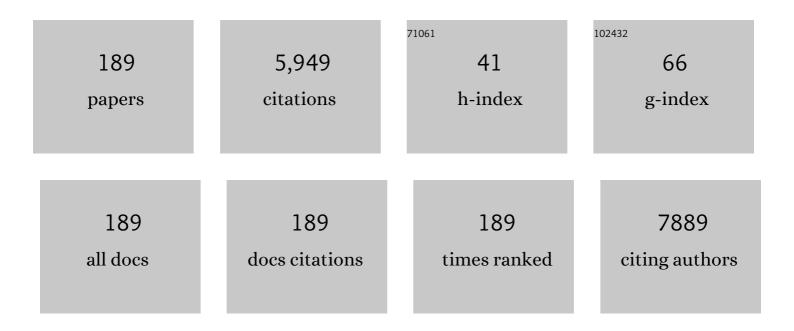
List of Publications by Year in descending order

Source: https://exaly.com/author-pdf/735380/publications.pdf Version: 2024-02-01



Δ7ΛΜ ΙΡΛΙΙ 7ΛΟ

#	Article	IF	CITATIONS
1	Enhanced Photoresponse and Wavelength Selectivity by SILAR-Coated Quantum Dots on Two-Dimensional WSe ₂ Crystals. ACS Omega, 2022, 7, 2091-2098.	1.6	9
2	Cauliflower-Like Ni/MXene-Bridged Fiber-Shaped Electrode for Flexible Microsupercapacitor. Energy & Fuels, 2022, 36, 2140-2148.	2.5	8
3	Three-dimensional hybrid of iron–titanium mixed oxide/nitrogen-doped graphene on Ni foam as a superior electrocatalyst for oxygen evolution reaction. Journal of Colloid and Interface Science, 2020, 563, 241-251.	5.0	13
4	ZIF-8/PEDOT @ flexible carbon cloth electrode as highly efficient electrocatalyst for oxygen reduction reaction. International Journal of Hydrogen Energy, 2020, 45, 1890-1900.	3.8	29
5	Development of a quartz crystal microbalance biodetector based on cellulose nanofibrils (CNFs) for glycine. Journal of Materials Science: Materials in Electronics, 2020, 31, 17451-17460.	1.1	2
6	Room temperature and high response ethanol sensor based on two dimensional hybrid nanostructures of WS2/GONRs. Scientific Reports, 2020, 10, 14799.	1.6	23
7	AC characterization of three-dimensional reduced graphene oxide/molybdenum disulfide nanorose hybrids for ethanol vapor detection. Applied Surface Science, 2020, 520, 146346.	3.1	1
8	Room temperature selective sensing of aligned Ni nanowires using impedance spectroscopy. Materials Research Express, 2020, 7, 025044.	0.8	6
9	A graphene/TiS3 heterojunction for resistive sensing of polar vapors at room temperature. Mikrochimica Acta, 2020, 187, 117.	2.5	14
10	Optimization of CuIn _{1–<i>X</i>} Ga _{<i>X</i>} S ₂ Nanoparticles and Their Application in the Hole-Transporting Layer of Highly Efficient and Stable Mixed-Halide Perovskite Solar Cells. ACS Applied Materials & Interfaces, 2019, 11, 30838-30845.	4.0	35
11	Iranian female faculties in physics. AIP Conference Proceedings, 2019, , .	0.3	Ο
12	<p>Doxorubicin/Cisplatin-Loaded Superparamagnetic Nanoparticles As A Stimuli-Responsive Co-Delivery System For Chemo-Photothermal Therapy</p> . International Journal of Nanomedicine, 2019, Volume 14, 8769-8786.	3.3	36
13	On the performance of vertical MoS2 nanoflakes as a gas sensor. Vacuum, 2019, 167, 90-97.	1.6	37
14	A Highâ€Performance and Lowâ€Cost Ethanol Vapor Sensor Based on a TiS ₂ /PVP Composite. ChemistrySelect, 2019, 4, 6662-6666.	0.7	8
15	A new co-solvent assisted CuSCN deposition approach for better coverage and improvement of the energy conversion efficiency of corresponding mixed halides perovskite solar cells. Journal of Materials Science: Materials in Electronics, 2019, 30, 11576-11587.	1.1	8
16	Shedding Light on Pseudocapacitive Active Edges of Single-Layer Graphene Nanoribbons as High-Capacitance Supercapacitors. ACS Applied Energy Materials, 2019, 2, 3665-3675.	2.5	18
17	High-Photoresponsive Backward Diode by Two-Dimensional SnS ₂ /Silicon Heterostructure. ACS Photonics, 2019, 6, 728-734.	3.2	24
18	Application of combinative TiO2nanorods and nanoparticles layer as the electron transport film in highly efficient mixed halides perovskite solar cells. Electrochimica Acta, 2019, 297, 1071-1078.	2.6	12

#	Article	IF	CITATIONS
19	Flexible and Mechanically Durable Asymmetric Supercapacitor Based on NiCo‣ayered Double Hydroxide and Nitrogenâ€Doped Graphene Using a Simple Fabrication Method. Energy Technology, 2019, 7, 1801002.	1.8	23
20	Iron‑vanadium oxysulfide nanostructures as novel electrode materials for supercapacitor applications. Journal of Electroanalytical Chemistry, 2018, 818, 157-167.	1.9	23
21	Communication—Scanning Kelvin Probe Study of Electrodeposited Nanostructured Cu ₂ 0/Perovskite Interfaces. ECS Journal of Solid State Science and Technology, 2018, 7, P60-P62.	0.9	1
22	Characterization of three-dimensional reduced graphene oxide/copper oxide heterostructures for hydrogen sulfide gas sensing application. Journal of Alloys and Compounds, 2018, 740, 1024-1031.	2.8	25
23	An efficient two-step approach for improvement of graphene aerogel characteristics in preparation of supercapacitor electrodes. Journal of Energy Storage, 2018, 17, 465-473.	3.9	49
24	Cadmium telluride quantum dots induce apoptosis in human breast cancer cell lines. Toxicology and Industrial Health, 2018, 34, 339-352.	0.6	31
25	Scanning tunneling spectroscopy of MoS2 monolayer in presence of ethanol gas. Materials Research Express, 2018, 5, 045022.	0.8	1
26	Investigating the different conditions on solution processed MoOx thin film in long lifetime fluorescent polymer light emitting diodes. Materials Chemistry and Physics, 2018, 204, 262-268.	2.0	4
27	Highly sensitive nonenzymetic glucose sensing platform based on MOF-derived NiCo LDH nanosheets/graphene nanoribbons composite. Journal of Electroanalytical Chemistry, 2018, 808, 114-123.	1.9	107
28	Transition metal ions-doped polyaniline/graphene oxide nanostructure as high performance electrode for supercapacitor applications. Journal of Solid State Electrochemistry, 2018, 22, 983-996.	1.2	32
29	Reproducible electrochemical analysis of nanostructured Cu2O using a non-aqueous 3-methoxypropionitrile-based electrolyte. Electrochemistry Communications, 2018, 86, 1-5.	2.3	3
30	Hydrogen sensing properties of nanocomposite graphene oxide/Co-based metal organic frameworks (Co-MOFs@GO). Nanotechnology, 2018, 29, 015501.	1.3	20
31	Photoluminescence and electrochemical investigation of curcumin-reduced graphene oxide sheets. Journal of the Iranian Chemical Society, 2018, 15, 351-357.	1.2	10
32	Simple Oneâ€Step Fabrication of Semiconductive Lateral Heterostructures Using Bipolar Electrodeposition. Physica Status Solidi - Rapid Research Letters, 2018, 12, 1800418.	1.2	13
33	Computational investigation of gas detection and selectivity on TiS3 nanoflakes supported by experimental evidence. Physical Chemistry Chemical Physics, 2018, 20, 25458-25466.	1.3	3
34	Ternary nanostructures of Cr2O3/graphene oxide/conducting polymers for supercapacitor application. Journal of Electroanalytical Chemistry, 2018, 823, 505-516.	1.9	78
35	Sensing behavior of flower-shaped MoS ₂ nanoflakes: case study with methanol and xylene. Beilstein Journal of Nanotechnology, 2018, 9, 608-615.	1.5	30
36	Silver Fiber Fabric as the Current Collector for Preparation of Graphene- Based Supercapacitors. Electrochimica Acta, 2017, 227, 246-254.	2.6	19

#	Article	IF	CITATIONS
37	Tunable bandgap and spin-orbit coupling by composition control of MoS 2 and MoO x (x = 2 and 3) thin film compounds. Materials and Design, 2017, 122, 220-225.	3.3	32
38	High Performance, Low Cost Electromechanical Systems Based on Electrostatically Actuated TiS2Belts. ChemistrySelect, 2017, 2, 3739-3743.	0.7	1
39	One step electrodeposition of V2O5/polypyrrole/graphene oxide ternary nanocomposite for preparation of a high performance supercapacitor. International Journal of Hydrogen Energy, 2017, 42, 21073-21085.	3.8	82
40	A new approach to flexible humidity sensors using graphene quantum dots. Journal of Materials Chemistry C, 2017, 5, 8966-8973.	2.7	56
41	Glassy carbon electrode modified with 3D graphene–carbon nanotube network for sensitive electrochemical determination of methotrexate. Sensors and Actuators B: Chemical, 2017, 239, 617-627.	4.0	111
42	Different buckling regimes in direct electrospinning: A comparative approach to rope buckling. Journal of Polymer Science, Part B: Polymer Physics, 2016, 54, 451-456.	2.4	5
43	H2S gasochromic effect of mixed ammonium salts of phosphomolybdate nanoparticles synthesized by microwave assisted technique. Sensors and Actuators B: Chemical, 2016, 237, 715-723.	4.0	4
44	Detecting hydrogen using graphene quantum dots/WO ₃ thin films. Materials Research Express, 2016, 3, 116407.	0.8	26
45	Hierarchical core–shell structure of ZnO nanotube/MnO ₂ nanosheet arrays on a 3D graphene network as a high performance biosensing platform. RSC Advances, 2016, 6, 61190-61199.	1.7	11
46	Graphene/cobalt nanocarrier for hyperthermia therapy and MRI diagnosis. Colloids and Surfaces B: Biointerfaces, 2016, 146, 271-279.	2.5	57
47	Electrical bending instability in electrospinning viscoâ€elastic solutions. Journal of Polymer Science, Part B: Polymer Physics, 2016, 54, 1036-1042.	2.4	11
48	Facile one-pot synthesis of polytypic (wurtzite–chalcopyrite) CuGaS2. Applied Physics A: Materials Science and Processing, 2016, 122, 1.	1.1	7
49	Preparation of ZnO nanoparticles/Ag nanowires nanocomposites as plasmonic photocatalysts and investigation of the effect of concentration and diameter size of Ag nanowires on their photocatalytic performance. Journal of Alloys and Compounds, 2016, 664, 707-714.	2.8	40
50	Ethanol sensing properties of PVP electrospun membranes studied by quartz crystal microbalance. Measurement: Journal of the International Measurement Confederation, 2016, 78, 283-288.	2.5	29
51	Voltammetric studies of Azathioprine on the surface of graphite electrode modified with graphene nanosheets decorated with Ag nanoparticles. Materials Science and Engineering C, 2016, 58, 1098-1104.	3.8	39
52	Enhanced photoelectrochemical processes by interface engineering, using Cu 2 O nanorods. Materials Letters, 2016, 163, 81-84.	1.3	18
53	Improving the status of Iranian women in physics. AIP Conference Proceedings, 2015, , .	0.3	5
54	Flexible strain sensors based on electrostatically actuated graphene flakes. Journal of Micromechanics and Microengineering, 2015, 25, 075016.	1.5	8

#	Article	lF	CITATIONS
55	Sensitive and selective room temperature H2S gas sensor based on Au sensitized vertical ZnO nanorods with flower-like structures. Journal of Alloys and Compounds, 2015, 628, 222-229.	2.8	128
56	Synthesis and characterization of NiCo2O4 nanorods for preparation of supercapacitor electrodes. Journal of Solid State Electrochemistry, 2015, 19, 269-274.	1.2	94
57	One-pot thermolysis synthesis of CulnS2 nanoparticles with chalcopyrite-wurtzite polytypism structure. Journal of Materials Science: Materials in Electronics, 2015, 26, 8960-8972.	1.1	9
58	A new strategy on utilizing nitrogen doped TiO 2 in nanostructured solar cells: Embedded multifunctional N-TiO 2 scattering particles in mesoporous photoanode. Materials Research Bulletin, 2015, 72, 64-69.	2.7	11
59	Improved photovoltaic performance of nanostructured solar cells by neodymium-doped TiO2 photoelectrode. Materials Letters, 2015, 159, 273-275.	1.3	22
60	Nitrogen-doped submicron-size TiO2 particles as bifunctional light scatterers in dye-sensitized solar cells. Applied Physics A: Materials Science and Processing, 2015, 119, 1283-1290.	1.1	11
61	Mixed ammonium silver phosphomolybdate salt nanostructures; solid state synthesis, characterization of driving agent role and photocatalytic property. Materials Letters, 2015, 161, 464-467.	1.3	5
62	Synthesis and characterization of electrochemically grown CdSe nanowires with enhanced photoconductivity. Journal of Materials Science: Materials in Electronics, 2015, 26, 1395-1402.	1.1	11
63	Room temperature H2S gas sensor based on rather aligned ZnO nanorods with flower-like structures. Sensors and Actuators B: Chemical, 2015, 207, 865-871.	4.0	224
64	Influence of cathode roughness on the performance of F8BT based organic–inorganic light emitting diodes. Organic Electronics, 2015, 16, 87-94.	1.4	10
65	Structural and optical properties of Fe and Zn substituted CuInS ₂ nanoparticles synthesized by a one-pot facile method. Journal of Materials Chemistry C, 2015, 3, 889-898.	2.7	15
66	Defect study of TiO2 nanorods grown by a hydrothermal method through photoluminescence spectroscopy. Journal of Luminescence, 2015, 157, 235-242.	1.5	58
67	Simply synthesized TiO ₂ nanorods as an effective scattering layer for quantum dot sensitized solar cells. Chinese Physics B, 2014, 23, 047302.	0.7	14
68	Electromechanical resonators based on electrospun ZnO nanofibers. Journal of Micro/ Nanolithography, MEMS, and MOEMS, 2014, 13, 043011.	1.0	1
69	Graphene/PbS as a Novel Counter Electrode for Quantum Dot Sensitized Solar Cells. ACS Photonics, 2014, 1, 323-330.	3.2	52
70	Fabrication of gas ionization sensor based on titanium oxide nanotube arrays. Applied Physics A: Materials Science and Processing, 2014, 115, 1387-1393.	1.1	17
71	In-situ electro-polymerization of graphene nanoribbon/polyaniline composite film: Application to sensitive electrochemical detection of dobutamine. Sensors and Actuators B: Chemical, 2014, 196, 582-588.	4.0	45
72	Comparative study of the grown ZnO nanostructures on quartz and alumina substrates by vapor phase transport method without catalyst: Synthesis and acetone sensing properties. Sensors and Actuators A: Physical, 2014, 212, 80-86.	2.0	11

#	Article	IF	CITATIONS
73	A novel field ionization gas sensor based on self-organized CuO nanowire arrays. Sensors and Actuators A: Physical, 2014, 216, 202-206.	2.0	29
74	Pd–WO3/reduced graphene oxide hierarchical nanostructures as efficient hydrogen gas sensors. International Journal of Hydrogen Energy, 2014, 39, 8169-8179.	3.8	163
75	Growth control of cobalt oxide nanoparticles on reduced graphene oxide for enhancement of electrochemical capacitance. International Journal of Hydrogen Energy, 2014, 39, 21068-21075.	3.8	31
76	Electrochemical functionalization of graphene nanosheets with catechol derivatives as an effective method for preparation of highly performance supercapacitors. Electrochimica Acta, 2014, 147, 136-142.	2.6	17
77	Structural and Optical Study of Ga ³⁺ Substitution in CuInS ₂ Nanoparticles Synthesized by a One-Pot Facile Method. Journal of Physical Chemistry C, 2014, 118, 24670-24679.	1.5	29
78	Facile synthesis of gradient alloyed ZnxCd1â^'xS nanocrystals using a microwave-assisted method. Journal of Alloys and Compounds, 2014, 586, 380-384.	2.8	21
79	Optoelectronic properties of cauliflower like ZnO–ZnO nanorod/p-Si heterostructure. Solid-State Electronics, 2013, 80, 33-37.	0.8	10
80	DNA-decorated graphene nanomesh for detection of chemical vapors. Applied Physics Letters, 2013, 103, 183110.	1.5	45
81	An Artificial Neural Networks Model for Predicting Permeability Properties of Nano Silica–Rice Husk Ash Ternary Blended Concrete. International Journal of Concrete Structures and Materials, 2013, 7, 225-238.	1.4	19
82	Fabrication of Pd Doped WO3 Nanofiber as Hydrogen Sensor. Polymers, 2013, 5, 45-55.	2.0	44
83	Freestanding light scattering hollow silver spheres prepared by a facile sacrificial templating method and their application in dye-sensitized solar cells. Journal of Power Sources, 2013, 225, 46-50.	4.0	10
84	Enhanced electronic contacts in SnO2–dye–P3HT based solid state dye sensitized solar cells. Physical Chemistry Chemical Physics, 2013, 15, 2075.	1.3	17
85	Improved charge collection efficiency of hollow sphere/nanoparticle composite TiO2 electrodes for solid state dye sensitized solar cells. Current Applied Physics, 2013, 13, 371-376.	1.1	12
86	Pt and Pd as catalyst deposited by hydrogen reduction of metal salts on WO3 films for gasochromic application. Applied Surface Science, 2013, 273, 261-267.	3.1	26
87	Investigating the effects of using different types of SiO2 nanoparticles on the mechanical properties of binary blended concrete. Composites Part B: Engineering, 2013, 54, 52-58.	5.9	115
88	Electromechanical resonator based on electrostatically actuated graphene-doped PVP nanofibers. Nanotechnology, 2013, 24, 135201.	1.3	5
89	Synthesis and characterization of TiO2–graphene nanocomposites modified with noble metals as a photocatalyst for degradation of pollutants. Applied Catalysis A: General, 2013, 462-463, 82-90.	2.2	59
90	Effect of growth conditions on zinc oxide nanowire array synthesized on Si (100) without catalyst. Materials Science in Semiconductor Processing, 2013, 16, 171-178.	1.9	8

#	Article	IF	CITATIONS
91	H ₂ S Sensing Properties of Added Copper Oxide in WO ₃ . Key Engineering Materials, 2013, 543, 145-149.	0.4	1
92	Catalytic Effect of Copper Oxide on H ₂ S Sensing Properties of Nanostructured WO ₃ . Sensor Letters, 2013, 11, 2015-2020.	0.4	3
93	STRUCTURAL AND OPTICAL CHARACTERIZATION OF NANOCRYSTALLINE CuAIS2 CHALCOPYRITE SYNTHESIZED BY POLYOL METHOD IN AUTOCLAVE. International Journal of Modern Physics B, 2012, 26, 1250179.	1.0	3
94	UV photodetection of laterally connected ZnO rods grown on porous silicon substrate. Sensors and Actuators A: Physical, 2012, 180, 11-14.	2.0	41
95	The effect of operating temperature on gasochromic properties of amorphous and polycrystalline pulsed laser deposited WO3 films. Sensors and Actuators B: Chemical, 2012, 169, 284-290.	4.0	26
96	Colouration process of colloidal tungsten oxide nanoparticles in the presence of hydrogen gas. Applied Surface Science, 2012, 258, 10089-10094.	3.1	13
97	The decoration of TiO2/reduced graphene oxide by Pd and Pt nanoparticles for hydrogen gas sensing. International Journal of Hydrogen Energy, 2012, 37, 15423-15432.	3.8	130
98	An IPMC-made deformable-ring-like robot. Smart Materials and Structures, 2012, 21, 065011.	1.8	43
99	Easily manufactured TiO ₂ hollow fibers for quantum dot sensitized solar cells. Physical Chemistry Chemical Physics, 2012, 14, 522-528.	1.3	42
100	Fabrication of Sensitive Glutamate Biosensor Based on Vertically Aligned CNT Nanoelectrode Array and Investigating the Effect of CNTs density on the electrode performance. Analytical Chemistry, 2012, 84, 5932-5938.	3.2	86
101	New gasochromic system: nanoparticles in liquid. Journal of Nanoparticle Research, 2012, 14, 1.	0.8	17
102	Pd2+ reduction and gasochromic properties of colloidal tungsten oxide nanoparticles synthesized by pulsed laser ablation. Applied Physics A: Materials Science and Processing, 2012, 108, 401-407.	1.1	6
103	Effect of nanostructured electrode architecture and semiconductor deposition strategy on the photovoltaic performance of quantum dot sensitized solar cells. Electrochimica Acta, 2012, 75, 139-147.	2.6	62
104	Mediator-less highly sensitive voltammetric detection of glutamate using glutamate dehydrogenase/vertically aligned CNTs grown on silicon substrate. Biosensors and Bioelectronics, 2012, 31, 110-115.	5.3	29
105	Synthesis of sodium tungsten oxide nano-thick plates. Materials Letters, 2012, 82, 214-216.	1.3	25
106	Fluorine Treatment of TiO2 for Enhancing Quantum Dot Sensitized Solar Cell Performance. Journal of Physical Chemistry C, 2011, 115, 14400-14407.	1.5	105
107	Melatonin as a powerful bio-antioxidant for reduction of graphene oxide. Journal of Materials Chemistry, 2011, 21, 10907.	6.7	255
108	Micro helical polymeric structures produced by variable voltage direct electrospinning. Soft Matter, 2011, 7, 10548.	1.2	32

#	Article	IF	CITATIONS
109	Investigation on the dynamics of electron transport and recombination in TiO2 nanotube/nanoparticle composite electrodes for dye-sensitized solar cells. Physical Chemistry Chemical Physics, 2011, 13, 21487.	1.3	29
110	Comparative study of ZnO nanostructures grown on silicon (100) and oxidized porous silicon substrates with and without Au catalyst by chemical vapor transport and condensation. Journal of Alloys and Compounds, 2011, 509, 4295-4299.	2.8	16
111	Growth of ZnO Nanostructures on Porous Silicon and Oxidized Porous Silicon Substrates. Brazilian Journal of Physics, 2011, 41, 113-117.	0.7	9
112	Palladium nanoparticle deposition onto the WO3 surface through hydrogen reduction of PdCl2: Characterization and gasochromic properties. Solar Energy Materials and Solar Cells, 2011, 95, 2335-2340.	3.0	52
113	Fabrication of self-organised highly ordered titanium oxide nanotube arrays by anodic oxidation and characterisation. International Journal of Nanomanufacturing, 2010, 5, 297.	0.3	о
114	Design and fabrication of sensitive carbon nanotubes/PMMA film for acetone vapour detection. International Journal of Nanomanufacturing, 2010, 5, 268.	0.3	3
115	Photocatalytic activity of ZnO nanoparticles prepared viaÂsubmerged arc discharge method. Applied Physics A: Materials Science and Processing, 2010, 100, 1097-1102.	1.1	41
116	Investigation of hydrogen sensing properties and aging effects of Schottky like Pd/porous Si. Sensors and Actuators B: Chemical, 2010, 146, 53-60.	4.0	27
117	Electroless plating of palladium on WO3 films for gasochromic applications. Solar Energy Materials and Solar Cells, 2010, 94, 201-206.	3.0	44
118	On the Formation of TiO2 Nanoparticles Via Submerged Arc Discharge Technique: Synthesis, Characterization and Photocatalytic Properties. Journal of Cluster Science, 2010, 21, 753-766.	1.7	37
119	Comparison of Trapâ€state Distribution and Carrier Transport in Nanotubular and Nanoparticulate TiO ₂ Electrodes for Dye‣ensitized Solar Cells. ChemPhysChem, 2010, 11, 2140-2145.	1.0	45
120	Synthesis and characterization of alumina flakes/polymer composites. Journal of Applied Polymer Science, 2010, 115, 3716-3720.	1.3	5
121	Fabrication of gas ionization sensor using carbon nanotube arrays grown on porous silicon substrate. Sensors and Actuators A: Physical, 2010, 162, 24-28.	2.0	35
122	Pd doped WO3 films prepared by sol–gel process for hydrogen sensing. International Journal of Hydrogen Energy, 2010, 35, 854-860.	3.8	133
123	Hydrogen sensing properties of multi-walled carbon nanotube films sputtered by Pd. International Journal of Hydrogen Energy, 2010, 35, 4445-4449.	3.8	28
124	Density functional theory prediction for oxidation and exfoliation of graphite to graphene. Applied Surface Science, 2010, 256, 7596-7599.	3.1	15
125	Mechanical properties of graphene cantilever from atomic force microscopy and density functional theory. Nanotechnology, 2010, 21, 185503.	1.3	63
126	Strain effect on quantum conductance of graphene nanoribbons from maximally localized Wannier functions. Physical Review B, 2010, 81, .	1.1	34

#	Article	IF	CITATIONS
127	Electrochemically Assisted Photocatalytic Oxidation of Methanol on TiO2 Nanotube Arrays. Journal of Materials Science and Technology, 2010, 26, 535-541.	5.6	15
128	TiO2nanotubular fibers sensitized with CdS nanoparticles. EPJ Applied Physics, 2010, 50, 20601.	0.3	13
129	ZnO nanoparticles prepared by electrical arc discharge method in water. Materials Chemistry and Physics, 2009, 118, 6-8.	2.0	72
130	Rapid and efficient synthesis of colloidal gold nanoparticles byÂarc discharge method. Applied Physics A: Materials Science and Processing, 2009, 96, 423-428.	1.1	32
131	Field emission of Co nanowires in polycarbonate template. Thin Solid Films, 2009, 517, 1736-1739.	0.8	13
132	Cu surface segregation in Ni/Cu system. Vacuum, 2009, 84, 469-473.	1.6	5
133	Comparison of various anodization and annealing conditions of titanium dioxide nanotubular film on MB degradation. EPJ Applied Physics, 2009, 47, 10601.	0.3	14
134	Stability, size and optical properties of colloidal silver nanoparticles prepared by electrical arc discharge in water. EPJ Applied Physics, 2009, 48, 10601.	0.3	26
135	Hybrid multiwalled carbon nanotubes and trioxide tungsten nanoparticles for hydrogen gas sensing. Journal Physics D: Applied Physics, 2009, 42, 165105.	1.3	27
136	Two-Dimensional Clustering of Nanoparticles on the Surface of Cellulose Fibers. Journal of Physical Chemistry C, 2009, 113, 12022-12027.	1.5	1
137	Morphology and hydrogen sensing studies of the electrodeposited nanostructure palladium on porous silicon. International Journal of Nanotechnology, 2009, 6, 892.	0.1	1
138	CdO/PSi/Si photo detector. International Journal of Nanotechnology, 2009, 6, 997.	0.1	2
139	Real-time measurement of oxidation dynamics ofÂsub-stoichiometric tungsten oxide films by pulsed laser deposition. Applied Physics A: Materials Science and Processing, 2008, 92, 627-634.	1.1	10
140	Enhanced inter-plane coupling of Mg doped Cu0.5Tl0.5Ba2Ca2â^'xMgxCu3O10â^'δ superconductors: XPS and FTIR studies. Physica C: Superconductivity and Its Applications, 2008, 468, 405-410.	0.6	10
141	Fourier transform infrared spectroscopy and scanning tunneling spectroscopy of porous silicon in the presence of methanol. Sensors and Actuators B: Chemical, 2008, 132, 40-44.	4.0	16
142	Self-assembled one-pot synthesis of red luminescent CdS:Mn/Mn(OH)2 nanoparticles. Journal of Luminescence, 2008, 128, 1980-1984.	1.5	16
143	The effect of Pd addition to Fe as catalysts on growth of carbon nanotubes by TCVD method. Applied Surface Science, 2008, 254, 6416-6421.	3.1	17
144	Pulsed laser deposition of W–V–O composite films: Preparation, characterization and gasochromic studies. Solar Energy Materials and Solar Cells, 2008, 92, 878-883.	3.0	55

#	Article	IF	CITATIONS
145	Gasochromic tungsten oxide thin films for optical hydrogen sensors. Journal Physics D: Applied Physics, 2008, 41, 055405.	1.3	25
146	Surface plasmon resonance of two-segmented Au–Cu nanorods. Nanotechnology, 2008, 19, 415705.	1.3	4
147	Synthesis and photocatalytic activity of WO ₃ nanoparticles prepared by the arc discharge method in deionized water. Nanotechnology, 2008, 19, 195709.	1.3	115
148	Thermochemical growth of Mn-doped CdS nanoparticles and study of luminescence evolution. Nanotechnology, 2008, 19, 225705.	1.3	21
149	Palladium Plating on Macroporous/Microporous Silicon: Application as a Hydrogen Sensor. Synthesis and Reactivity in Inorganic, Metal Organic, and Nano Metal Chemistry, 2007, 37, 377-380.	0.6	8
150	The effect of grain size on the fluctuation-induced conductivity of Cu1â´'xTlxBa2Ca3Cu4O12â´´l´superconductor thin films. Superconductor Science and Technology, 2007, 20, 742-747.	1.8	29
151	Hydrogen Sensing Properties of Pure and Pd Activated WO3 Nanostructured Films. Synthesis and Reactivity in Inorganic, Metal Organic, and Nano Metal Chemistry, 2007, 37, 453-456.	0.6	12
152	Time dependence of the surface plasmon resonance of copper nanorods. Journal of Physics Condensed Matter, 2007, 19, 446007.	0.7	10
153	Diffusion and segregation of substrate copper in electrodeposited Ni–Fe thin films. Journal of Alloys and Compounds, 2007, 443, 81-86.	2.8	18
154	Adsorption of TiO2Nanoparticles on Glass Fibers. Journal of Physical Chemistry C, 2007, 111, 9794-9798.	1.5	21
155	Characterization of Pd nanoparticle dispersed over porous silicon as a hydrogen sensor. Journal Physics D: Applied Physics, 2007, 40, 7201-7209.	1.3	45
156	The Effect of Oxidation of Macroporous Silicon on Carbon Nanotubes Growth by TCVD Method. Synthesis and Reactivity in Inorganic, Metal Organic, and Nano Metal Chemistry, 2007, 37, 489-492.	0.6	4
157	Synthesis of Titania Nanofibers for Photocatalytic Applications. Synthesis and Reactivity in Inorganic, Metal Organic, and Nano Metal Chemistry, 2007, 37, 457-460.	0.6	5
158	An optical study of cobalt nanowires dispersed in liquid phase. Optics Communications, 2007, 274, 471-476.	1.0	6
159	Etched glass surfaces, atomic force microscopy and stochastic analysis. Physica A: Statistical Mechanics and Its Applications, 2007, 375, 239-246.	1.2	22
160	X-ray photoemission studies of Zn doped Cu1â^'xTlxBa2Ca2Cu 3â^'yZnyO10â^'δ (y=0, 2.65) superconductors. Physica C: Superconductivity and Its Applications, 2007, 453, 46-51.	0.6	14
161	GMR in multilayered nanowires electrodeposited in track-etched polyester and polycarbonate membranes. Journal of Magnetism and Magnetic Materials, 2007, 308, 35-39.	1.0	53
162	Size, composition and optical properties of copper nanoparticles prepared by laser ablation in liquids. Applied Physics A: Materials Science and Processing, 2007, 88, 415-419.	1.1	197

#	Article	IF	CITATIONS
163	The effect of liquid environment on size and aggregation of gold nanoparticles prepared by pulsed laser ablation. Journal of Nanoparticle Research, 2007, 9, 853-860.	0.8	49
164	X-ray photo-emission studies of Cu1â^'xTlxBa2Ca3Cu4O12â^'y superconductor thin films. Physica C: Superconductivity and Its Applications, 2006, 449, 47-52.	0.6	13
165	Structure and composition of the segregated Cu in V2O5/Cu system. Applied Surface Science, 2006, 253, 2581-2588.	3.1	1
166	On the growth sequence of highly ordered nanoporous anodic aluminium oxide. Materials & Design, 2006, 27, 983-988.	5.1	52
167	Effective factors on Pd growth on porous silicon by electroless-plating: Response to hydrogen. Sensors and Actuators B: Chemical, 2006, 115, 164-169.	4.0	34
168	Scanning tunneling spectroscopy of porous silicon in presence of methanol. Sensors and Actuators B: Chemical, 2006, 120, 172-176.	4.0	4
169	The effect of the Cr and Mo on the surface accumulation of copper in the electrodeposited Ni–Fe/Cu alloy films. Materials Science and Engineering B: Solid-State Materials for Advanced Technology, 2006, 127, 17-21.	1.7	11
170	Stability, size and optical properties of silver nanoparticles prepared by laser ablation in different carrier media. Applied Physics A: Materials Science and Processing, 2006, 84, 215-219.	1.1	186
171	Itinerant electron transport in microscopically inhomogeneous magnetic fields. Journal of Magnetism and Magnetic Materials, 2006, 299, 356-361.	1.0	8
172	Fine tuning of the size of CdS nanoparticles synthesized by a photochemical method. Nanotechnology, 2006, 17, 1230-1235.	1.3	24
173	Photo-induced CdS nanoparticles growth. Physica E: Low-Dimensional Systems and Nanostructures, 2005, 30, 114-119.	1.3	22
174	XPS studies of Cu1â^'xTlxBa2Ca2Cu3O10â^'y superconductor thin films. Physica C: Superconductivity and Its Applications, 2005, 433, 21-27.	0.6	8
175	The effect of target annealing temperature on optical and structural properties and composition of CdS thin films prepared by pulsed laser. Optical Materials, 2005, 27, 1583-1586.	1.7	12
176	Characterization of etched glass surfaces by wave scattering. Surface and Interface Analysis, 2005, 37, 641-645.	0.8	25
177	The effect of the Cr and Mo on the physical properties of electrodeposited Ni–Fe alloy films. Journal of Alloys and Compounds, 2005, 386, 43-46.	2.8	24
178	Characterization of porous poly-silicon impregnated with Pd as a hydrogen sensor. Journal Physics D: Applied Physics, 2005, 38, 36-40.	1.3	39
179	A photochemical method for controlling the size of CdS nanoparticles. Nanotechnology, 2005, 16, 334-338.	1.3	55
180	Two-scale Kirchhoff theory: comparison of experimental observations with theoretical prediction. Journal of Statistical Mechanics: Theory and Experiment, 2005, 2005, P04013.	0.9	11

#	Article	IF	CITATIONS
181	STUDYING OF POROUS POLY-SILICON IN PRESENCE OF ETHANOL BY SCANNING TUNNELING SPECTROSCOPY. , 2005, , .		0
182	Characterization of porous poly-silicon as a gas sensor. Sensors and Actuators B: Chemical, 2004, 100, 341-346.	4.0	38
183	Stochastic Analysis and Regeneration of Rough Surfaces. Physical Review Letters, 2003, 91, 226101.	2.9	100
184	Height fluctuations and intermittency of V2O5films by atomic force microscopy. Journal of Physics Condensed Matter, 2003, 15, 1889-1898.	0.7	17
185	Room temperature diffusion of Cu in vanadium pentoxide thin films. Journal Physics D: Applied Physics, 2002, 35, 1176-1182.	1.3	6
186	Thermal desorption of ultrathin silicon oxide layers on Si(111). Semiconductor Science and Technology, 2000, 15, 160-163.	1.0	5
187	Low temperature conductivity of ultra thin deposits of Ag on Ge(100). Solid State Communications, 1992, 83, 467-471.	0.9	18
188	Electrical transport properties of thin Ni films subjected to an array of nanomagnets. , 0, , .		0
189	Bimetallic Oxide Nanosheets from Nickel–Vanadium Layered Double Hydroxide as an Efficient Cathode for Rechargeable Nickel–Zinc Batteries. Energy & Fuels, 0, , .	2.5	3